



# Absorbing aerosols and pre-summer monsoon hydroclimate variability over the Indian subcontinent: The challenge in investigating links

Massimo Bollasina\*, Sumant Nigam

Department of Atmospheric and Oceanic Science, 3417 Computer and Space Science Building, University of Maryland, College Park, MD 20742-2425, United States

## ARTICLE INFO

### Article history:

Received 23 March 2009

Received in revised form 2 June 2009

Accepted 17 June 2009

### Keywords:

Absorbing aerosols

Pre-monsoon hydroclimate

## ABSTRACT

The sub-monthly evolution of the interannual variations of absorbing aerosols and related hydrometeorology over South Asia in the pre-monsoon period is investigated from the analysis of pentad-resolution observational datasets.

It is shown that pre-monsoon (late April–early May) variations are characterized by increased aerosols, reduced cloudiness and precipitation, and increased downward shortwave radiation. Lead-lag regressions indicate the significant influence of synoptic scale advection (and related vertical motion) in *simultaneously* shaping the aerosol distribution and associated significant hydroclimate (precipitation, cloudiness, surface shortwave radiation, and 2-m air temperature) over the Indo-Gangetic Plain.

The above findings can be interpreted as a manifestation of the aerosol “semi-direct” effect if one is not mindful of the prevailing circulation anomalies and their concurrent impact on aerosol and hydroclimate. The complex interplay among aerosols, dynamics and precipitation also shows the challenge of extracting the aerosol impact from an observational analysis. Finally, the analysis points to the pitfalls of a columnar, circulation-blind framework in investigating aerosol–monsoon interactions, a concern of relevance in analyses of the impact of long-term aerosol trends, as well.

© 2009 Elsevier B.V. All rights reserved.

## 1. Introduction

Over the past decade there has been a substantial improvement in the knowledge of the amount, geographical distribution, physical and chemical properties of atmospheric aerosols. Intensive field experiments, new surface and remote-sensing observations, and improved representation of aerosol processes in models have shed new insights into the controlling mechanisms, radiative effects, and the influence of aerosols on climate.

The influence of anthropogenic aerosols on the Earth's radiation budget is however still considered the largest uncertainty in radiative forcing under climate change (IPCC, 2007). The quantification of tropospheric aerosol effects is challenging because of their large spatial and temporal

variability, diverse physical and chemical properties, and complex interactions of aerosols with radiation, microphysical processes and circulation (e.g., Ramanathan et al., 2001; Menon, 2004; Lohmann and Feichter, 2005). The influence of large-scale circulation on both aerosol distribution and regional hydroclimate is an additional complicating factor in the analysis of aerosol effects – one emphasized in this study.

A number of observational studies have characterized the South Asian aerosol cloud (e.g., Eck et al., 2001; Hsu et al., 2003; Ramanathan and Ramana, 2005; Dey and Tripathi, 2007; Gautam et al., 2007; Prasad and Singh, 2007; Ramachandran and Cherian, 2008), a 3-km thick brown layer persisting from October to May from the Himalayan foothills to the northern Indian Ocean, with a large contribution to aerosol optical depth from absorbing aerosols (e.g., dust (12%) and black carbon (11%); Ramanathan et al., 2001). This haze induces a large perturbation to the radiative energy budget of the region (up to  $-25 \text{ Wm}^{-2}$  in the mean clear-sky surface radiation; Ramanathan et al., 2005) which has

\* Corresponding author. Tel.: +1 240 565 1192.

E-mail address: [massimo@atmos.umd.edu](mailto:massimo@atmos.umd.edu) (M. Bollasina).

significant implications for the water budget, agriculture and health. Understanding the effects of aerosols on the distribution and duration of the South Asian monsoon rainfall (which accounts for nearly 75% of the yearly precipitation over many regions of the subcontinent) would be relevant for more than 60% of the world's population.

The large-scale impact of aerosols on the monsoon, mostly its climatological rainfall distribution, has been addressed by general circulation modeling studies (Menon et al., 2002; Ramanathan et al., 2005; Chung and Ramanathan, 2006; Lau et al., 2006; Meehl et al., 2008; Randles and Ramaswamy, 2008) and several mechanisms have been proposed (e.g., Ramanathan and Carmichael, 2008). Despite the usefulness of climate models in highlighting the physical processes and the mechanisms involved in the aerosol–monsoon interaction, some caution is necessary in interpreting the results, as these models are known to have significant biases in the climatological distribution and evolution of monsoon precipitation (e.g., Dai, 2006; Bollasina and Nigam, 2008). Furthermore, aerosol effects are only partially represented in many models (e.g., Kiehl, 2007), and large uncertainties are associated even with those effects currently included (e.g., Kinne et al., 2006).

Reanalysis and remote-sensed gridded observational datasets have been recently analyzed by Lau and Kim (2006) and, somewhat more comprehensively, by Bollasina et al. (2008) (hereafter BNL). In particular, BNL showed interannual variations of absorbing aerosols over the Indo-Gangetic Plain (IGP) in late spring to have a large-scale impact on the development of the ensuing summer monsoon through aerosol-induced anomalies of cloudiness (the “semi-direct” effect; Hansen et al., 1997) and the mediation of land–surface processes: reduced cloudiness (and rainfall) over the IGP in May associated with high aerosol loading leads to heating of the land surface and development of a low-level cyclonic circulation that brought more rain to northeastern India in May, and to western peninsular India in June.

However, the coarse-resolution monthly data used in BNL did not allow a close temporal investigation of the development of aerosol anomalies and of the evolution of their linkages with atmospheric and surface anomalies. This motivated the present work.

This study analyzes observational data at a higher temporal resolution (i.e., five-day averages (pentads) instead of monthly data) and focuses on the transition period prior to the monsoon onset. The goal was to describe the evolution of aerosol-related anomalies in radiative and hydrometeorological fields in order to better pinpoint aerosol effects. Indeed, the analysis showed the IGP aerosols to lead large-scale anomalies over the Indian Subcontinent starting by the end of April and for several pentads. However, the identification of mechanisms at play and aerosol effects, per se, is shown to be challenging given the dominant role played by the large-scale low-level horizontal advection and associated vertical circulation. In this view, caution is necessary in attributing causes and effects if one is not cognizant of the orchestrating role of the large-scale low-level circulation.

The paper is organized as follows: data and methods used in the analysis are described in Section 2. Section 3 examines the variability of absorbing aerosols over India and associated links with the large-scale pre-monsoon conditions. Concluding remarks follow in Section 4.

## 2. Datasets

Several independent datasets were used in this study. The loading of absorbing aerosols was characterized by means of

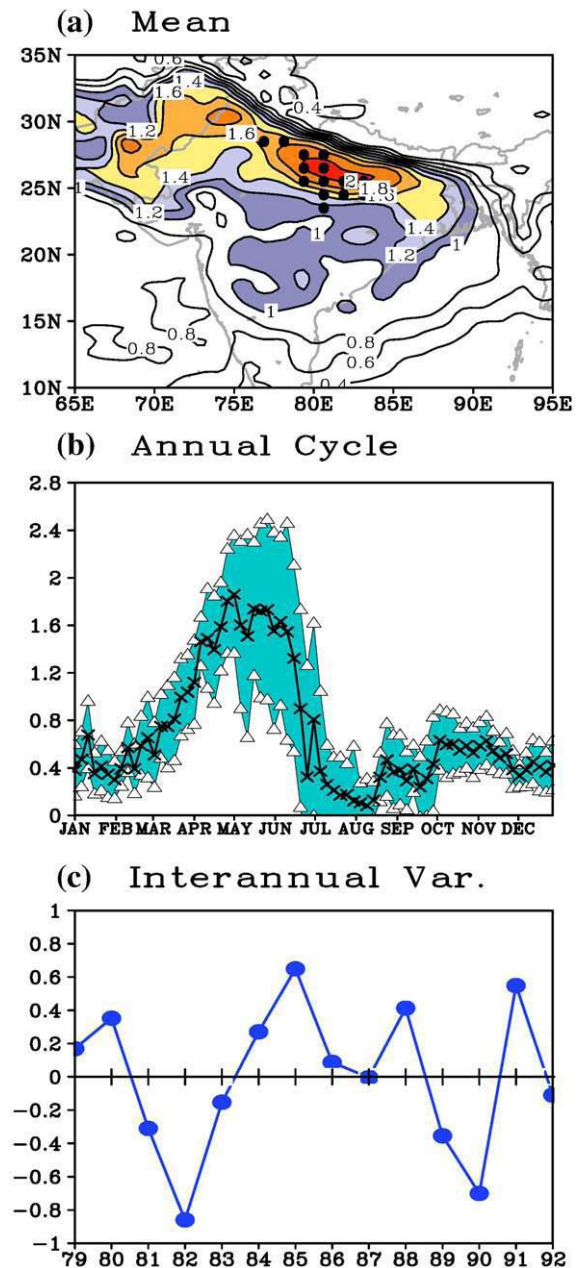


**Fig. 1.** Characteristics of the absorbing aerosol layer based on the TOMS AI (dimensionless) during the period 1979–1992: (a) the mean spatial distribution for the three-pentad period 26 April–10 May; (b) climatological annual cycle (crossed line), with the range of plus/minus one standard deviation around the mean enclosed by the shaded area, averaged over region marked with black points in (a); (c) time series of anomalies (averaged between 26 April–10 May and after removing the linear trend, which is  $0.042 \text{ yr}^{-1}$ ) averaged over the same region of (b). The points marked in (a) are consistent with Bollasina et al. (2008) and correspond to the locations of highest interannual variability (standard deviation greater than 0.5). (For interpretation of the references to colour in this figure legend, the reader is referred to the web version of this article.)

daily values of the Total Ozone Mapping Spectrometer (TOMS) Aerosol Index (AI), available on a  $1.25^\circ \times 1^\circ$  grid from November 1978 onwards (Torres et al., 2002). As discussed in BNL, several issues limited the length of the time series used in this analysis to the period 1979–1992.

The European Center for Medium-range Weather Forecasts (ECMWF) Reanalysis (ERA-40; Uppala et al., 2005) provided 6-

hourly atmospheric and surface data on a  $2.5^\circ \times 2.5^\circ$  grid. Observed precipitation came from the Global Precipitation Climatology Project (GPCP) pentad dataset, available on a  $2.5^\circ \times 2.5^\circ$  grid from 1979 (Adler et al., 2003). Daily surface shortwave radiation and total cloud fraction data were obtained from the Global Energy and Water Cycle Experiment (GEWEX) Surface Radiation Budget (SRB) Project at  $1^\circ$  resolution from

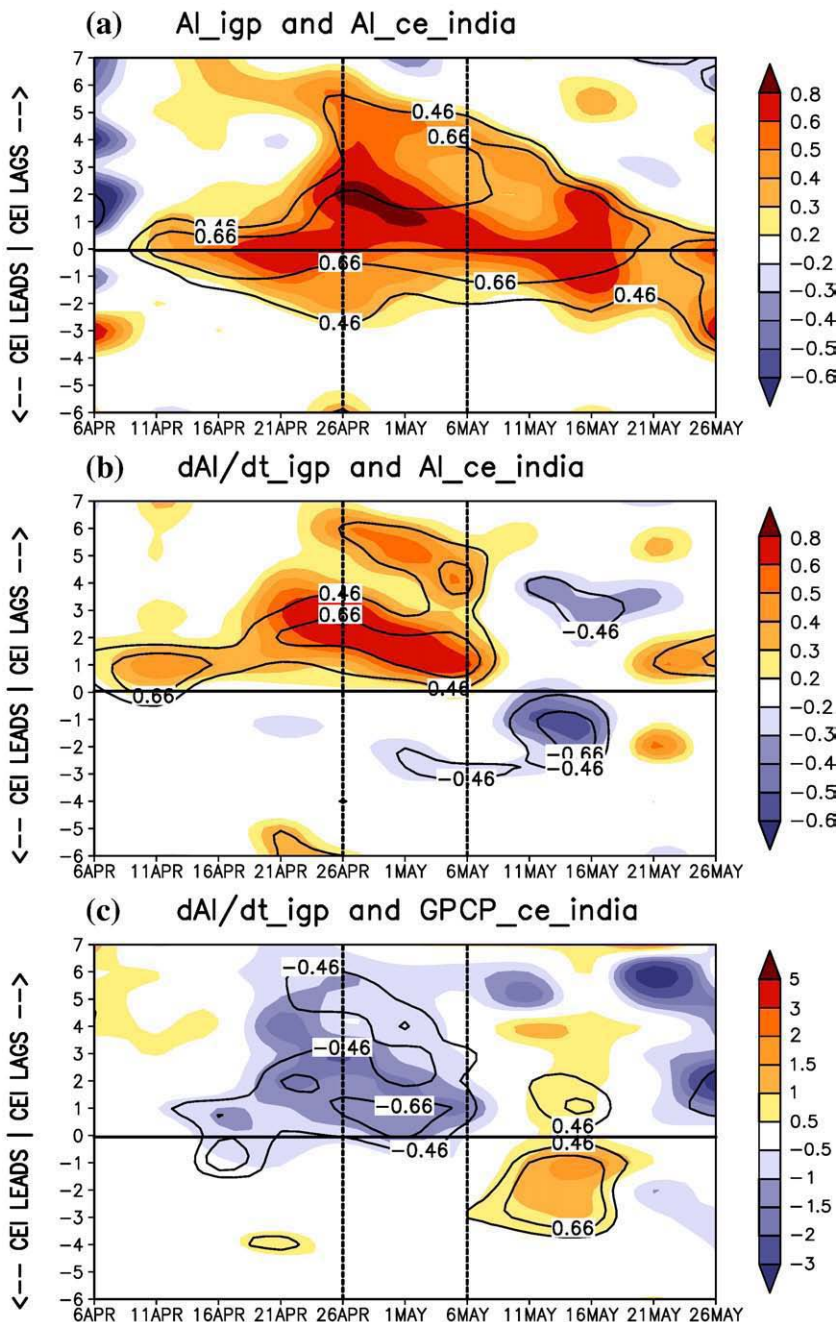


**Fig. 2.** Time evolution of central-eastern India (CEI) anomalies (shaded) of aerosols ((a) and (b); dimensionless) and precipitation ((c);  $\text{mm day}^{-1}$ ) lead/lag regressed on (a) the aerosol time series and (b) and (c) the aerosol tendency time series over the IGP (defined in Fig. 1b). The  $\pm 0.46$  and  $\pm 0.66$  contour lines show the 90% and 99% confidence levels, respectively. The x-axis is the reference pentad of the IGP anomalies, the y-axis is the lead/lag (negative/positive) of CEI anomalies with respect to IGP anomalies in terms of number of pentads. The horizontal line denotes the zero-lag axis, while the dotted vertical lines highlight the period 26 April–6 May.

January 1984 onward (Gupta et al., 1999). The National Oceanic and Atmospheric Administration (NOAA) daily outgoing long-wave radiation (OLR) data on a  $2.5^\circ \times 2.5^\circ$  grid (Liebmann and Smith, 1996) were also used.

All data were averaged over pentad intervals (starting every year on January 1), and correlations/regressions were computed using linearly detrended time series of anomalies (with respect to the 1979–1992 mean annual cycle) in order

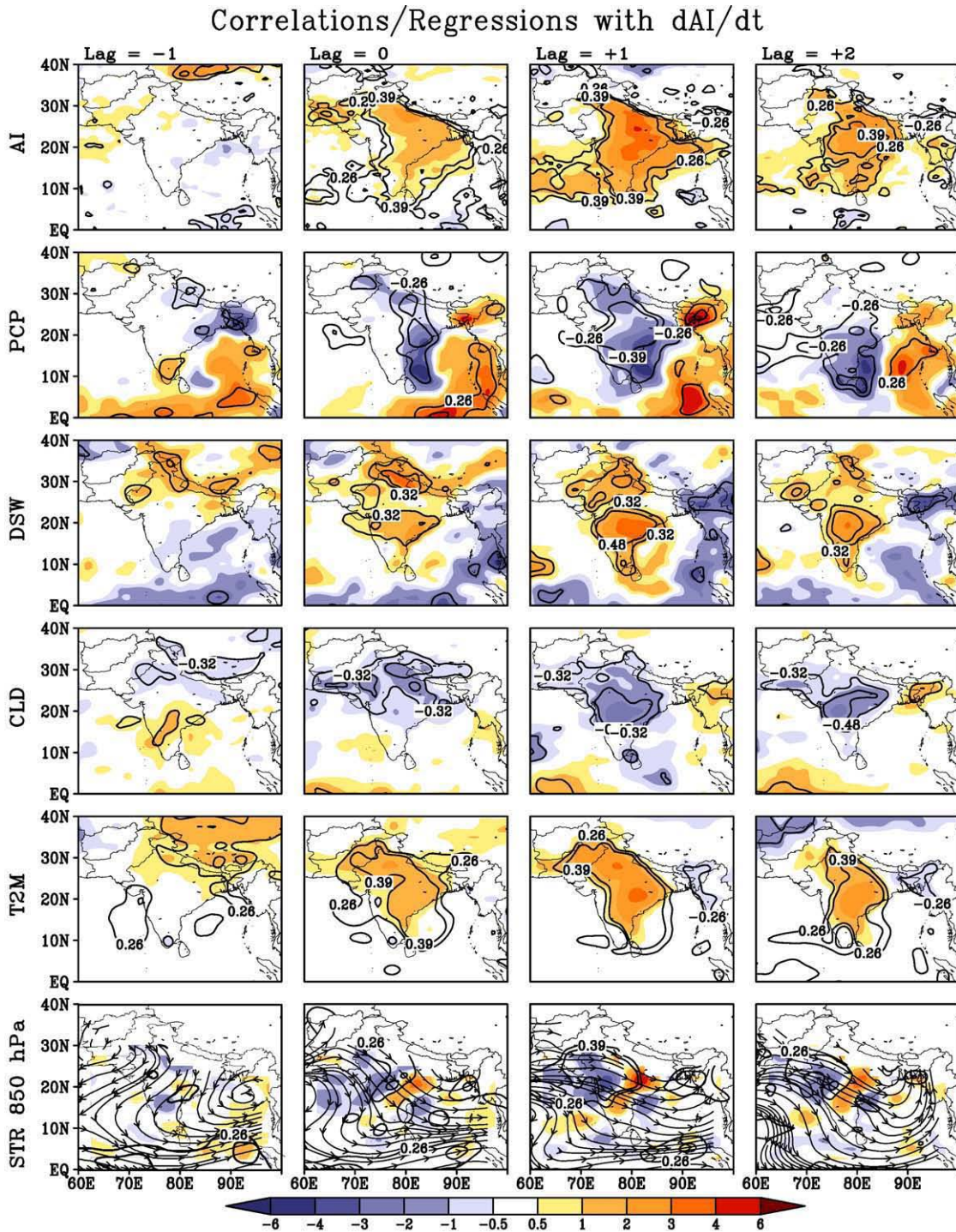


**Fig. 3.** Aerosols (AI, dimensionless), precipitation (PCP,  $\text{mm day}^{-1}$ ), downward shortwave radiation (DSW,  $\text{W m}^{-2}$ ), total cloudiness (CLD, fraction), 2-m air temperature (T2M,  $^\circ\text{C}$ ), 850-hPa streamlines (STR) and convergence ( $\text{s}^{-1}$ , shaded) regressed on the aerosol tendency time series over the IGP at different lead/lags during 1979–1992 (1984–1992 for cloudiness and radiation). The base period (lag 0) is the three-pentad period 26 April–10 May. The  $\pm 0.26$  ( $\pm 0.32$ ) and  $\pm 0.39$  ( $\pm 0.48$ ) contour lines show the 90% and 99% confidence levels, respectively.

to minimize the influence of trends on the strength of the deduced relationships. Pentad averaging is effective in masking out the day-to-day fluctuations of weather while retaining the sub-monthly variability arising from the super-synoptic time-scale processes in the atmosphere – the component of interest here.

### 3. Results

The fundamental characteristics of absorbing aerosols over the Indian Subcontinent are summarized in Fig. 1. The climatological distribution during 26 April–10 May – a three-pentad period corresponding to peak aerosol loading over most parts of India – is shown in Fig. 1a. The aerosol cloud is clearly piled up against the Himalayan foothills, and has a distinct maximum over the IGP with northwestward extension towards Pakistan. Climatologically, the lower-tropospheric subsidence over northwestern India associated with westerly flow across Afghanistan and Pakistan plays a major role in building up the aerosol layer during spring (e.g., Dey et al., 2004). Dust storms are common in the Middle East and the Thar Desert in late spring and early summer, and they are an effective dust source for the Indian subcontinent because of the prevailing westerlies. The IGP is one of the most densely populated basins in the world and the large emission of regional pollutants from fossil fuels (typically invariant through the season) and biomass burning (predominant in winter and spring) also contributes to the total aerosol loading (e.g., Habib et al., 2006).

The solid dots marked in Fig. 1a delineate the region used in defining the aerosol time series, consistently with BNL. The dots mark the locations of the highest interannual variability of aerosols (standard deviation of TOMS AI greater than 0.5), and the resulting time series of the areally averaged aerosol anomalies (referred to as the “IGP aerosol time series”) is thus an efficient marker of the aerosol signal. Lead/lag regressions of the sub-continental atmospheric circulation on this regional aerosol time series are used to characterize the aerosol-related anomalies. The seasonal evolution of the detrended time series is displayed in Fig. 1b. The pentad data shows the rapid buildup of aerosols in late spring and a precipitous drop in June due to the monsoon onset – features not discernible in monthly data (cf. Fig. 1e in BNL). The aerosol loading peaks in the first pentad of May (i.e., 1–5 May). The envelope around the seasonal curve marks the range of variability at plus/minus one standard deviation. The interannual variability is evidently much larger in late spring and early summer (i.e., in the pre-monsoon onset period) than at other times.

The detrended record of the IGP aerosol anomalies averaged over three pentads (26 April–10 May) is shown in Fig. 1c, the linear trend in the 1979–1992 period being  $+0.042 \text{ yr}^{-1}$ . The time series displayed in Fig. 1c is used in the following regression analysis.

Fig. 2 displays the lead/lag regressions and correlations of the IGP aerosol anomalies with aerosols over central-eastern India (Fig. 2a), and of the IGP aerosol tendency (computed as centered differences of the aerosol anomalies) with aerosols and precipitation of the same region (Fig. 2b and c, respectively). Central-eastern India, as defined here, includes the core of the Indian peninsula and, referring to the

homogeneous monsoon rainfall divisions of the Indian Institute of Tropical Meteorology, encloses the west central, central northeast (up to  $85^\circ\text{E}$ ), and the peninsular (to  $15^\circ\text{N}$ ) divisions. The IGP aerosol time series exhibits a certain amount of autocorrelation at all times (not shown) since aerosol loading is maintained by the eastward advection of dust and local emissions, resulting in a residence time of the order of one pentad. Fig. 2a shows that IGP aerosols are strongly linked with the aerosol loading over central-eastern India (a downstream region, see bottom panels in Fig. 3) from the end of April to mid-May, especially at  $+2$ – $3$  pentad lag (i.e., IGP aerosols leading by  $2$ – $3$  pentads), indicating a role for large-scale advection in the aerosol buildup over the latter region. The advection link is consistent with Fig. 2b, which shows the lead/lag relationship of the IGP aerosol tendency. A positive tendency is linked with increased aerosol anomalies over central-eastern India  $2$ – $3$  pentads later, but uncorrelated with antecedent anomalies of the same region.

The lead/lag links of the tendency of a quantity (as above) generally highlight the high-frequency response (Cayan, 1992). These links are often more pertinent as the tendency, rather than the quantity itself, is part of the related prognostic equation. Fig. 2c shows positive AI-tendency over the IGP region to be negatively linked with precipitation over central-eastern India in late April and early May. The negative correlations originate at lag 0 and persist for several (positive) lags. This pattern may indicate an influence of aerosols on the atmosphere. However, the similar delay in aerosol-increase and precipitation-decrease over central-eastern India suggests that either one pentad is a too long interval for discerning cause and effect or an orchestrating role for the large-scale circulation (shown later in Fig. 3).

The lead/lag links of aerosol tendency, aerosols, and precipitation over the same region (e.g., central-eastern India) are similar to those depicted in Fig. 2, and thus not shown. The aerosol tendency is anticipated to lead aerosols, but not precipitation, necessarily. For instance, aerosol-washout will manifest as negative contemporaneous correlation, in the absence of other influences. The negative correlations in Fig. 2c (and in a corresponding figure where all quantities are for central-eastern India, not shown) are however strongest at lag  $+2$  pentads, suggesting that washout alone is not the major process, although it may well be important in conjunction with other processes (e.g., aerosol advection).

The relationship between the regional aerosol variability (viz. the IGP aerosol tendency) and the larger-scale circulation and hydroclimate variability is shown in Fig. 3 with respect to the base period of 26 April–10 May, when the IGP aerosols have pronounced delayed links. Mean spatial patterns during this three-pentad period are shown at various lead/lags, beginning with the distribution of absorbing aerosols themselves. Not surprisingly, the IGP AI-tendency is linked with the aerosol buildup which is striking across the  $\pm$  one pentad lag/lead regressions. The buildup is not confined to the north central region (covered by solid dots in Fig. 1a) but is more expansive, covering much of the Subcontinent over a two-pentad period. The buildup evidently persists, at least for one more pentad (i.e., lag  $+2$ ). The direction of the buildup (southeastward) and its delayed nature indicate a significant role of the large-scale circulation, especially advection.

The correlations between precipitation and AI-tendency show diminished precipitation, especially to the south of the core aerosol buildup. The lack of collocation is noteworthy, and indicative of the significance of processes that generate a nonlocal hydroclimate response to aerosol loading, or of the role of circulation (advection and convergence) in modulating both aerosol loadings and precipitation. The next three variables – downward surface shortwave radiation, total cloudiness fraction, and 2-m air temperature – obtained from independent data sets, paint a coherent picture showing aerosol buildup and diminished precipitation to be linked with reduced cloudiness, more surface shortwave radiation, and higher 2-m temperature (and reduced convection, as manifested in the OLR anomalies, not shown here). While a physically consistent scenario emerges, the attribution remains challenging for reasons mentioned earlier. For instance, both diminished precipitation (from non-aerosol influence) and aerosol buildup can initiate the displayed sequences, the latter mechanism being envisioned through its semi-direct effect. Interestingly, both effects can be simultaneously generated by the large-scale flow, blowing from the dry and dusty desert regions to the west/northwest. Regardless of the instigating mechanism, this analysis indicates that aerosol buildup is accompanied by more surface shortwave radiation, suggesting that cloudiness fluctuations can easily overwhelm the surface radiation shortfall due to aerosol absorption.

The 850-hPa anomalous circulation (not plotted in the Himalayan foothills to avoid the use of fictitious, below-ground values), especially the northwesterly-to-westerly flow, argues for the importance of advection (and horizontal convergence) in the aerosol buildup, which is also indicated by the rapidity of the buildup (cf. top panel). The advective contribution is further shaped by related vertical motions (not shown). A comparison of 850 hPa convergence (Fig. 3, bottom panels) and aerosol distributions indicates that convergence can be influential (e.g., at lag + 1).

#### 4. Concluding remarks

The sub-monthly evolution of the interannual variations of absorbing aerosols and related hydrometeorological conditions over South Asia in the pre-monsoon period is investigated using pentad-resolution observational datasets during the period 1979–1992. This study was motivated by the findings of Bollasina et al. (2008) on the linkage between anomalous aerosol build up in May and delayed rainfall onset, based on the analysis of the monthly data. The delayed onset was attributed to the aerosol “semi-direct” effect and the ensuing land–atmosphere interactions. The initial goal of this study was to uncover the process sequence underlying aerosol–climate interactions. However, the present analysis indicates the challenge of an observationally-based approach.

The pentad-resolution analysis portrays a complex picture of aerosol evolution over central-eastern India, in which circulation plays a significantly role. The pervasive influence of advection precludes a robust analysis of the aerosol impact. Removal of the advective contribution is reasonably straightforward in the case of aerosol loading, but not for many other meteorological parameters that interact with aerosols (e.g., cloudiness and precipitation).

The late April to early May variations are characterized by aerosol loadings in central-eastern India lagging the build up in the northern plains. Anomalous aerosols are shown to be associated with significant anomalies of surface and atmospheric variables over the Indian Subcontinent. The precipitation evolution is nearly synchronous but not collocated with the aerosol build up core. Cloudiness, surface shortwave radiation, and 2-m air temperature evolve in concert, precluding attribution of the noted changes.

The extraction of the aerosol impact is very challenging, observationally, in large measure because of the significant influence of large-scale advection and horizontal divergence in shaping the aerosol distribution as well as regional hydroclimate. For instance, the spatiotemporal evolution displayed in Fig. 3 – specifically, aerosol-increase, reduced cloudiness and precipitation, and increased downward shortwave radiation – can be reasonably interpreted as the manifestation of the aerosol “semi-direct” effect, or equally, of the influence of reduced precipitation (from non-aerosol causes), if one were not mindful of the concurrent circulation anomalies. Inspection of the low-level flow structure as well as its horizontal convergence however suggests that all the above effects can just as well arise, simultaneously, from the evolving synoptic scale flow and related hydrometeorology – pointing to the pitfalls of a columnar, circulation-blind analysis framework.

Regardless of the instigation mechanism, it is shown that the aerosol buildup is accompanied by more surface shortwave radiation associated with cloudiness reduction, suggesting that cloudiness fluctuation can be as relevant as surface radiation shortfall due to aerosol absorption. This point is important for modeling studies of absorbing aerosol effects on climate, especially considering model deficiencies in realistically simulating cloud changes and feedbacks (e.g., Randall et al., 2007).

This pentad-resolution analysis of the anomalous aerosol evolution in the pre-monsoon-onset period indicates a prominent role for low-level circulation advection (and related vertical motions) in modulating the aerosol loadings, both mechanistically and through related meteorology. The role of large-scale circulation in modulating aerosol loading (and related impacts) may be appreciable even in the context of decadal variability and longer-term trends in regional hydroclimate.

#### Acknowledgements

The authors acknowledge NSF and DOE support through ATM-0649666 and DEFG0208ER64548 grants.

#### References

- Adler, R.F., et al., 2003. The Version 2 Global Precipitation Climatology Project (GPCP) monthly precipitation analysis (1979–present). *J. Hydrometeorol.* 4, 1147–1167.
- Bollasina, M., Nigam, S., 2008. Indian Ocean SST, evaporation, and precipitation during the South Asian summer monsoon in IPCC-AR4 coupled simulations. *Clim. Dyn.* doi:10.1007/s00382-008-0477-4.
- Bollasina, M., Nigam, S., Lau, K.-M., 2008. Absorbing aerosols and summer monsoon evolution over South Asia: an observational portrayal. *J. Clim.* 21, 3221–3239.
- Cayan, D.R., 1992. Latent and sensible heat flux anomalies over the northern oceans: driving the sea surface temperature. *J. Phys. Oceanogr.* 22, 859–881.

- Chung, C.E., Ramanathan, V., 2006. Weakening of North Indian SST gradients and the monsoon rainfall in India and the Sahel. *J. Clim.* 19, 2036–2045.
- Dai, A., 2006. Precipitation characteristics in eighteen coupled climate models. *J. Clim.* 19, 4605–4630.
- Dey, S., Tripathi, S.N., 2007. Estimation of aerosol optical properties and radiative effects in the Ganga basin, northern India, during the wintertime. *J. Geophys. Res.* 112, D03203. doi:10.1029/2006JD007267.
- Dey, S., Tripathi, S.N., Singh, R.P., 2004. Influence of dust storms on the aerosol optical properties over the Indo-Gangetic basin. *J. Geophys. Res.* 109, doi:1029/2004JD004924.
- Eck, T.F., Holben, B.N., Dubovik, O., Smirnov, A., Slutsker, I., Lobert, J.M., Ramanathan, V., 2001. Column integrated aerosol optical properties over the Maldives during the northeast monsoon for 1998–2000. *J. Geophys. Res.* 106, 28555–28566.
- Gautam, R., Hsu, N.C., Kafatos, M., Tsay, S.-C., 2007. Influences of winter haze on fog/low cloud over the Indo-Gangetic plains. *J. Geophys. Res.* 112, D05207. doi:10.1029/2005JD007036.
- Gupta, S.K., Ritchey, N.A., Wilber, A.C., Whitlock, C.H., Gibson, G.G., Stackhouse, P.W., 1999. A climatology of surface radiation budget derived from satellite data. *J. Clim.* 12, 2691–2710.
- Habib, G., Venkataraman, C., Chiappello, I., Ramachandran, S., Boucher, O., Reddy, M.S., 2006. Seasonal and interannual variability in absorbing aerosols over India derived from TOMS: relationship to regional meteorology and emissions. *Atmos. Environ.* 40, 1909–1921. doi:10.1016/j.atmosenv.2005.07.077.
- Hansen, J., Sato, M., Ruedy, R., 1997. Radiative forcing and climate response. *J. Geophys. Res.* 102 (D6), 6831–6864.
- Hsu, N.C., Herman, J.R., Tsay, S.C., 2003. Radiative impacts from biomass burning in the presence of clouds during boreal spring in Southeast Asia. *Geophys. Res. Lett.* 30, 1224. doi:10.1029/2002GL016485.
- IPCC, 2007. *Climate Change 2007: The Physical Science Basis. Contribution of Working Group I to the Fourth Assessment Report of the Intergovernmental Panel on Climate Change*. In: Solomon, S., Qin, D., Manning, M., Chen, Z., Marquis, M., Averyt, K.B., Tignor, M., Miller, H.L. (Eds.), Cambridge University Press, Cambridge, United Kingdom and New York, NY, USA, 996 pp.
- Kiehl, J.T., 2007. Twentieth century climate model response and climate sensitivity. *Geophys. Res. Lett.* 34, L22710. doi:10.1029/2007GL031383.
- Kinne, S., et al., 2006. An AeroCom initial assessment optical properties in aerosol component modules of global models. *Atmos. Chem. Phys.* 6, 1815–1834.
- Lau, K.-M., Kim, K.-M., 2006. Observational relationships between aerosol and Asian monsoon rainfall, and circulation. *Geophys. Res. Lett.* 33, L21810. doi:10.1029/2006GL027546.
- Lau, K.-M., Kim, M.K., Kim, K.-M., 2006. Aerosol induced anomalies in the Asian summer monsoon – the role of the Tibetan Plateau. *Clim. Dyn.* 26, 855–864. doi:10.1007/s00382-006-0114-z.
- Liebmann, B., Smith, C.A., 1996. Description of a complete (interpolated) outgoing longwave radiation dataset. *Bull. Am. Meteorol. Soc.* 77, 1275–1277.
- Lohmann, U., Feichter, J., 2005. Global indirect aerosol effects: a review. *Atmos. Chem. Phys.* 5, 715–737.
- Meehl, G.A., Arblaster, J.M., Collins, W.D., 2008. Effects of black carbon aerosols on the Indian monsoon. *J. Climate* 21, 2869–2882.
- Menon, S., Hansen, J., Nazarenko, L., Luo, Y., 2002. Climate effects of black carbon aerosols in China and India. *Science* 297, 2250–2253.
- Menon, S., 2004. Current uncertainties in assessing aerosol effects on climate. *Annu. Rev. Environ. Resour.* 29, 1–30.
- Prasad, A.K., Singh, R.P., 2007. Changes in aerosol parameters during major dust storm events (2001–2005) over the Indo-Gangetic Plains using AERONET and MODIS data. *J. Geophys. Res.* 112, D09208. doi:10.1029/2006JD007778.
- Ramachandran, S., Cherian, R., 2008. Regional and seasonal variations in aerosol optical characteristics and their frequency distributions over India during 2001–2005. *J. Geophys. Res.* 113, D08207. doi:10.1029/2007JD008560.
- Ramanathan, V., Ramana, M.V., 2005. Persistent, widespread, and strongly absorbing haze over the Himalayan foothills and the Indo-Ganges plains. *Pure Appl. Geophys.* 162, 1609–1626.
- Ramanathan, V., et al., 2001. Indian Ocean experiment: an integrated analysis of the climate forcing and effects of the great Indo-Asian haze. *J. Geophys. Res.* 106 (D22), 28371–28398.
- Ramanathan, V., et al., 2005. Atmospheric brown clouds: impacts on South Asian climate and hydrological cycle. *Proc. Natl. Acad. Sci. USA* 102, 5326–5333.
- Ramanathan, V., Carmichael, G., 2008. Global and regional change due to black carbon. *Nature Geosci.* 1, 221–227.
- Randall, D.A., Wood, R.A., Bony, S., Colman, R., Fife, T., Fyfe, J., Kattsov, V., Pitman, A., Shukla, J., Srinivasan, J., Stouffer, R.J., Sumi, A., Taylor, K.E., 2007. Climate models and their evaluation. In: Solomon, S., Qin, D., Manning, M., Chen, Z., Marquis, M.C., Averyt, K.B., Tignor, M., Miller, H.L. (Eds.), *Climate Change 2007: The Physical Science Basis. Contribution of Working Group I to the Fourth Assessment Report of the Intergovernmental Panel on Climate Change*.
- Randles, C.A., Ramaswamy, V., 2008. Absorbing aerosols over Asia: a geophysical fluid dynamics laboratory general circulation model sensitivity study of model response to aerosol optical depth and aerosol absorption. *J. Geophys. Res.* 113, D21203. doi:10.1029/2008JD010140.
- Torres, O., Bhartia, P.K., Herman, J.R., Sinyuk, A., Ginoux, P., Holben, B., 2002. A long-term record of aerosol optical depth from TOMS observations and comparison to AERONET measurements. *J. Atmos. Sci.* 59, 398–413.
- Uppala, S.M., et al., 2005. The ERA40 reanalysis. *Q. J. R. Meteorol. Soc.* 131, 2961–3012.